Experimental Observation of Two-Stage Melting in a Classical Two-Dimensional Screened Coulomb System

C. A. Murray and D. H. Van Winkle[a]

AT&T Bell Laboratories, Murray Hill, New Jersey 07974
(Received 6 October 1986)

We have observed a two-stage melting transition in a two-dimensional (2D) colloidal suspension of highly charged, submicron-sized spheres in water using optical microscopy and digital imaging. Our system is confined between two flat glass plates, has a lateral extent of at least 1000 spheres, and has equilibrated for over 10^5 time steps. Direct observation of topological defects and computed correlation functions from real-space images give insight into the nature of the 2D melting process.

Recently there has been much interest in the nature of the melting transition of 2D systems.[1] A spirited debate has raged for nearly a decade on the possible existence of the predicted Kosterlitz-Thouless-Halperin-Nelson-Young (KTHNY) melting process,[2-4] mediated by topological defects in a 2D solid. In the KTHNY theory, the system first makes a continuous transition associated with the unbinding of dislocation pairs from a crystalline state with algebraic decay of translational order and long-range orientational order to an intermediate "hexatic" phase that has algebraic decay of orientational order but exponential decay of translational order. The system subsequently makes another continuous transition associated with the unbinding of free dislocations into their substituent pairs of disclinations to a normal fluid with exponential decay of orientational as well as translational order. Several other theories[5,6] predict single first-order melting transitions in 2D. The search for the nature of the 2D melting transition has included numerous computer simulations on systems with various types of classical interactions[7,8] and experiments on systems such as liquid crystals,[9] noble gases physisorbed on substrates,[10] and electrons on He.[11]

Our experiment has many of the advantages of molecular-dynamics simulations, such as the ability to follow what is happening in real space and real time, but also avoids the problems in the numerical simulations created by periodic boundary conditions, a very small number of particles, and short equilibration times. Our sample consists of an ultraclean colloidal suspension of 0.305-μm ($\pm 2\%$) diameter polystyrene-sulphonate spheres[12] in 20°C water, confined between two smooth glass plates. The sphere charge as determined by pH is 20000 electrons. The experimental cell and procedures are described in detail elsewhere.[13] The spheres comprise a 2D system of particles interacting through screened Coulomb potentials, with perhaps a second-order quadrupole nature due to the image charges in the glass plates.

The spheres are repelled both by image charges and by surface charge on the glass plates, so that squeezing the plates closer together lowers the areal density of the spheres in between. A wedge of $(4 \pm 0.5) \times 10^{-4}$ rad is formed between the glass plates in the y direction, as depicted in the inset of Fig. 1. The wedge angle in the x direction is at least a factor of 5 smaller, so that the lateral extent of the colloid is ~ 1 mm, or ~ 1000 spheres. We use an optical microscope coupled with a digital charge-coupled–device camera to take 0.1-sec exposure snapshots of $\Delta x \times \Delta y = 38 \times 25$-$\mu$m^2 areas of the system along the wedge in the y direction. The locations of the sphere centers are determined to ± 1 pixel accuracy.
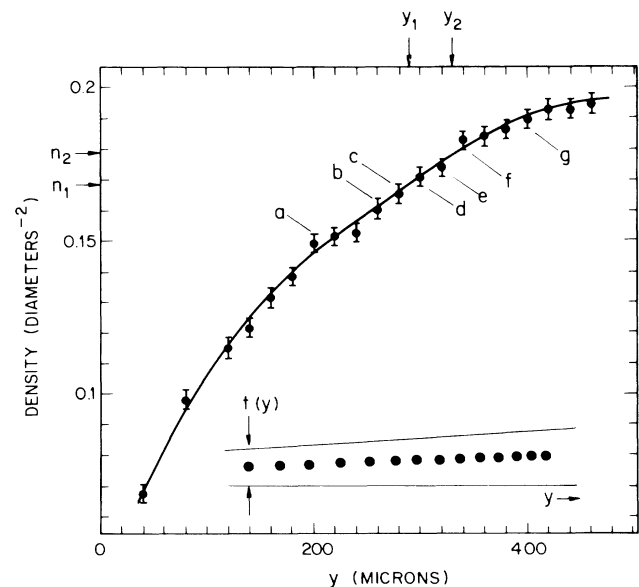

FIG. 1. Two-dimensional reduced density as a function of transition along the wedge y. Inset: Schematic drawing of the experimental wedge arrangement of colloid between two smooth glass plates. The thickness is $t(y=0)=1 \pm 0.3$ μm, and the wedge angle along y is $4 \pm 0.5 \times 10^{-4}$ rads. The wedge along the other lateral direction, x, is at least 5 times smaller. The two observed transitions, occurring at $y \sim 3.5$ diameters, are marked by arrows. The letters a–g mark various densities of interest.
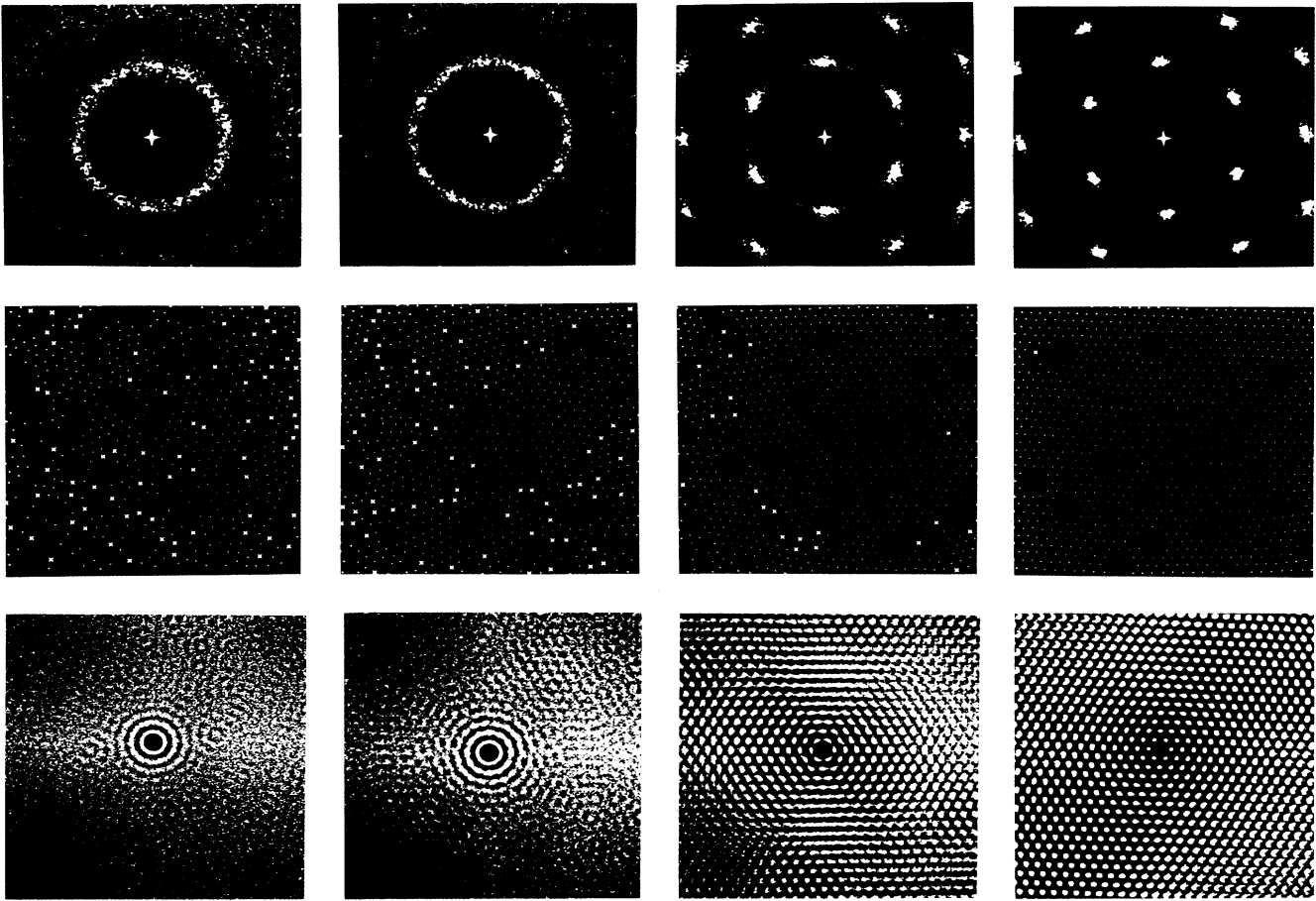
FIG. 2. Top: $S(K)$; center: locations of sphere centers; bottom: $g(r)$ computed from the series of images corresponding to the labels a, b, d, f in Fig. 1 with the density increasing left to right. For clarity, only about half of the complete image field is shown. Colors and shapes of the symbols used to represent sphere centers indicate their coordination as determined from a Voronoi polyhedron analysis. Blue diamond: 6, small red x: 5, and large yellow x: 7. The distance scales of the center and bottom rows are identical. The nearest-neighbor separations decrease from 0.85 μm to 0.76 μm from left to right.

The maximum number of spheres in an image is ~ 2000, for which the spheres are separated by ~ 10 pixels (0.67 μm). The use of the wedge geometry makes possible equilibration of the thin region of the sample with a 100-cm^3 3D reservoir in intimate contact with ion-exchange resin for long times and intimate contact of the 2D fluid and 2D crystal in the wedge. Consistent results were attained in five of seven different experimental runs, following > 1-month chemical equilibration after the change of a cell window, and > 20-hr mechanical equilibration after a small adjustment (~ 20 μm in thickness) to the wedge. The particle exchange time in the fluid is ~ 0.1 sec, so that the mechanical equilibration time necessary for consistency is $\sim 10^6$ exchange times. The areal reduced density of spheres, in units of (diameter)$^{-2}$, measured from a series of snapshots in one of these runs (~ 70 hr equilibration) is shown in Fig. 1.

Figure 2 shows the location of sphere centers in the images corresponding to the labels a, b, d, f in Fig. 1, the coordination of each sphere, determined by a Voronoi polyhedron construction,[14] and the computed structure factor, $S(K)$, and pair correlation function, $g(r)$, for these images. We have also computed the orientational correlation function[3]

$$g_6(r) = \langle \exp[-6i\theta(0)]\exp[-6i\theta(r)]\rangle/g_B(r),$$

where $g_B(r)$ is the pair correlation function of bond centers, and $\theta(r)$ is the angle with respect to the x axis of the bond whose center is located at r. In Fig. 3, the angular averages of $S(K)$, $g(r)$, and $g_6(r)$ are shown for the images corresponding to the labels $a-g$ in Fig. 1. The orientational correlation function changes from exponentially decaying on a scale of ~ 3 nearest-neighbor distances a_{nn} to a very long-range decaying function between curves c and d, and then becomes indistinguishable from constant at curve f. The translational correla-
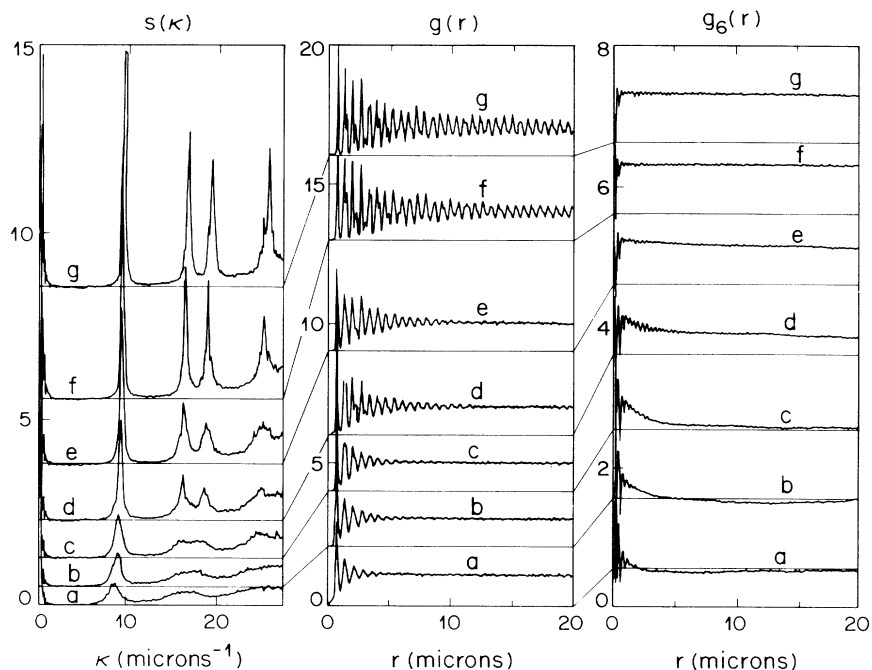
FIG. 3. Angular averages of $S(K)$ and translational and orientational correlation functions computed from the images corresponding to the labels $a-g$ in Fig. 1. Left: $S(K)$; center: $g(r)$; right: $g_6(r)$. Each successive curve is shifted vertically for clarity. The zero levels are marked by thin lines joining the curves associated with each density and extending beneath the plots.

tion length grows from $3a_{nn}$ to $5a_{nn}$ between c and d, but shoots up from $7a_{nn}$ to $\sim 30a_{nn}$ between e and f. We believe that these qualitative changes mark the existence of two distinct transitions in the system, at reduced densities of $n_1 = 0.168 \pm 0.003$ and $n_2 = 0.178 \pm 0.005$ in this run, arbitrarily estimated as the mean densities between successive images. The average densities determined in this way from the five equilibrated runs are $n_1 = 0.172 \pm 0.003$ and $n_2 = 0.181 \pm 0.003$, respectively. Each of the five runs includes 2–3 images in the intermediate phase, which spans a $(5 \pm 2)\%$ range in density. This intermediate phase bears the signature of the Halperin-Nelson[3] hexatic. The observed span in density can be compared to an 18% span found for the hexatic phase in a molecular-dynamics simulation of particles with $1/r$ repulsive interactions.[7]

In Fig. 4, the effective correlation lengths, determined by fits assuming exponential-decay envelopes for $g(r)$ and $g_6(r)$, are shown as functions of density. It is impossible to fit the $g(r)$ curves corresponding to densities below 0.182 (curve e) by power-law decay, but very good fits by power-law decay are obtained above that density. Good fits yield exponents of 0.09 ± 0.01 for curve e and 0.05 ± 0.01 for curve f. A good fit to $g_6(r)$ for curve d is a power law with decay of 0.15 ± 0.01. The largest exponent we have observed for $g_6(r)$ in all of the runs is 0.25 ± 0.01, just above n_1. Our observed exponents are consistent with the Halperin-Nelson predictions[3] of $< \frac{1}{3}$ and 0.25, respectively, just above the two

transitions.[15] Above density of 0.189, the correlation lengths for both translational and orientational order are reduced as a result of the approach to a second layer at
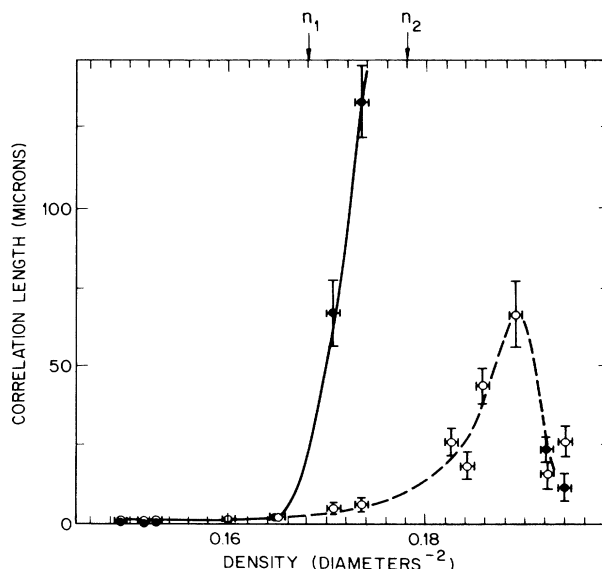

FIG. 4. Effective translational and orientational correlation lengths obtained from fits of exponentially decaying envelopes to $g(r)$ and $g_6(r)$ vs density. Open circles: translational correlational length; filled circles: orientational correlation lengths. Lines through the points are guides to the eye. The two phase transitions are marked by arrows.

$t \sim 1.2$ μm (with square symmetry[13]) in the system. We find that the general hexagonal symmetry of the lattice is not grossly perturbed, but that a network of grain boundaries separated by ~ 20–30 μm is introduced into the crystal.

The equilibrium dislocation concentration is 0.5% in the solid, and an estimate for the free energy of formation of dislocation cores is then 0.135 eV $(5.6k_BT)$, if we assume Boltzmann statistics. This is large compared to Chui's predicted cutoff of $2.84k_BT$ between strongly and weakly first-order transitions,[6] Saito's observations[16] of qualitatively different behavior in molecular-dynamics simulations of dislocation vector systems, and Strandburg's observed[17] crossover from first-order behavior to a hexatic phase in a Laplacian-roughening model.

Although all of the above are consistent with a picture of KTHNY melting in our experiment through two transitions and an intermediate hexatic phase, the nature of the topological defects in our experiment is considerably more complex than the simple KTHNY picture. We observe a considerable number of free disclinations in the low-density fluid (Fig. 2). In the high-density fluid near the hexatic, fourfold, fivefold, and sevenfold coordinated spheres merge into a network of grain boundaries surrounding regions of sixfold coordination that are on the order of $(3$–$5)a_{nn}$ in size, and randomly oriented with respect to neighboring regions of hexagonal symmetry. These small "grains" appear and disappear on the time scale of 1 sec. As the density is increased into the hexatic phase, the network of grain boundaries does not completely disappear, but instead, the neighboring grains begin to orient with respect to each other, leaving rows of vacancies and dislocations in between. In the low-density solid, we observe $\sim 1\%$ vacancies, an occasional dislocation bound to a vacancy, an occasional divacancy, and an occasional interstitial, but no bound pairs of dislocations.

In summary, we have observed a two-step melting transition in the 2D colloidal system with screened Coulomb interactions. The system melts through an intermediate phase with the signature of a hexatic. The dislocation core energy is found to be large enough to place the system into a KTHNY regime, yet the actual topological defects of the system are observed to be complex and are not consistent with a simple KTHNY picture of melting.

We would like to acknowledge fruitful conversations with D. S. Fisher, C. C. Grimes, B. I. Halperin, D. R. Nelson, and J. D. Weeks; software support by R. W. Lee; and help in the data reduction by J. Richardson.

(a)Present address: Physics Department, Florida State University, Tallahassee, Florida 32306.

[1]*Ordering in Two Dimensions,* edited by S. K. Sinha (North-Holland, Amsterdam, 1980).

[2]J. M. Kosterlitz and D. J. Thouless, J. Phys. C 6, 1181 (1973).

[3]B. I. Halperin and D. R. Nelson, Phys. Rev. B 19, 2457 (1979).

[4]A. P. Young, Phys. Rev. B 19, 1855 (1979).

[5]T. V. Ramkrishnan, Phys. Rev. Lett. 48, 541 (1982); H. Kleinert, Phys. Lett. 95A, 381 (1983); Y. E. Lozovik and V. M. Farztdinov, Solid State Commun. 54, 725 (1985).

[6]S. T. Chui, Phys. Rev. B 28, 178 (1973).

[7]V. M. Bedanov, G. V. Gadiyak, and Y. E. Lozovik, Zh. Eksp. Teor. Fiz. 88, 1622 (1985) [Sov. Phys. JETP 61, 967 (1985)].

[8]Hard disks: B. J. Alder and T. E. Wainwright, Phys. Rev. 127, 359 (1962); K. J. Strandburg, J. A. Zollweg, and G. V. Chester, Phys. Rev. B 30, 2755 (1984). Repulsive power law: J. P. McTague, D. Frenkel, and M. P. Allen, in Ref. 1, p. 147; J. Broughton, G. H. Gilmer, and J. D. Weeks, Phys. Rev. B 25, 4651 (1982); R. K. Kalia and P. Vashishta, J. Phys. C 14, L643 (1981); R. H. Morf, Phys. Rev. Lett. 43, 931 (1979); R. C. Gann, S. Chakravarty, and G. V. Chester, Phys. Rev. B 20, 326 (1979); R. W. Hockney and T. R. Brown, J. Phys. C 8, 1813 (1975). Lennard-Jones: A. F. Bakker, C. Bruin, and H. J. Hilhorst, Phys. Rev. Lett. 52, 449 (1984); J. Tobochnik and G. V. Chester, Phys. Rev. B 25, 6778 (1982); F. F. Abraham, Phys. Rev. Lett. 44, 463 (1980); D. Frenkel and J. P. McTague, Phys. Rev. Lett. 42, 1632 (1979). Logarithmic: A. T. Fiory, Phys. Rev. B 28, 236 (1983); P. Choquard and J. Clerouin, Phys. Rev. Lett. 50, 2086 (1983); J. M. Caillol, D. Levesque, J. J. Weis, and J. P. Hansen, J. Stat. Phys. 28, 325 (1982); S. W. de Leeuw and J. W. Perram, Physica (Amsterdam) 113A, 546 (1982). Gaussian: F. H. Stillinger and T. A. Weber, J. Chem. Phys. 74, 4015 (1981); T. A. Weber and F. H. Stillinger, J. Chem. Phys. 74, 4020 (1981).

[9]S. C. Davey, J. Budai, R. Pindak, and J. W. Goodby, Phys. Rev. Lett. 53, 2129 (1983).

[10]T. F. Rosenbaum, S. E. Nagler, P. M. Horn, and R. Clarke, Phys. Rev. Lett. 50, 1791 (1983); P. A. Heiney, R. J. Birgeneau, G. S. Brown, P. M. Horn, D. Moncton, and P. Stevens, Phys. Rev. Lett. 48, 104 (1982).

[11]C. C. Grimes and G. Adams, Phys. Rev. Lett. 42, 795 (1979); C. J. Guo, D. B. Mast, R. Mehrotra, Y. Z. Ruan, M. A. Stan, and A. J. Dahm, Phys. Rev. Lett. 51, 1461 (1983).

[12]Manufactured by the Dow Chemical Co., Midland, MI.

[13]D. H. Van Winkle and C. A. Murray, Phys. Rev. A 34, 562 (1986).

[14]G. F. Voronoi, J. Reine Agnew. Math. 134, 198 (1908); also see M. F. Ashby, F. Spapen, and S. Williams, Acta Metall. 26, 1647 (1978).

[15]As our images contain only ~ 2000 spheres, the fits by power laws for single images are uncertain because of the particle-number fluctuations ($\pm 2\%$) in equilibrium for single snapshots. Because we have such coarse graining in density in the experiment, we cannot make a distinction at this time as to the order of the two observed transitions. Also, since our sphere diameter and charge vary by as much as 2%, one would expect any first-order transition to be smeared out.

[16]Y. Saito, Phys. Rev. B 26, 6239 (1982).
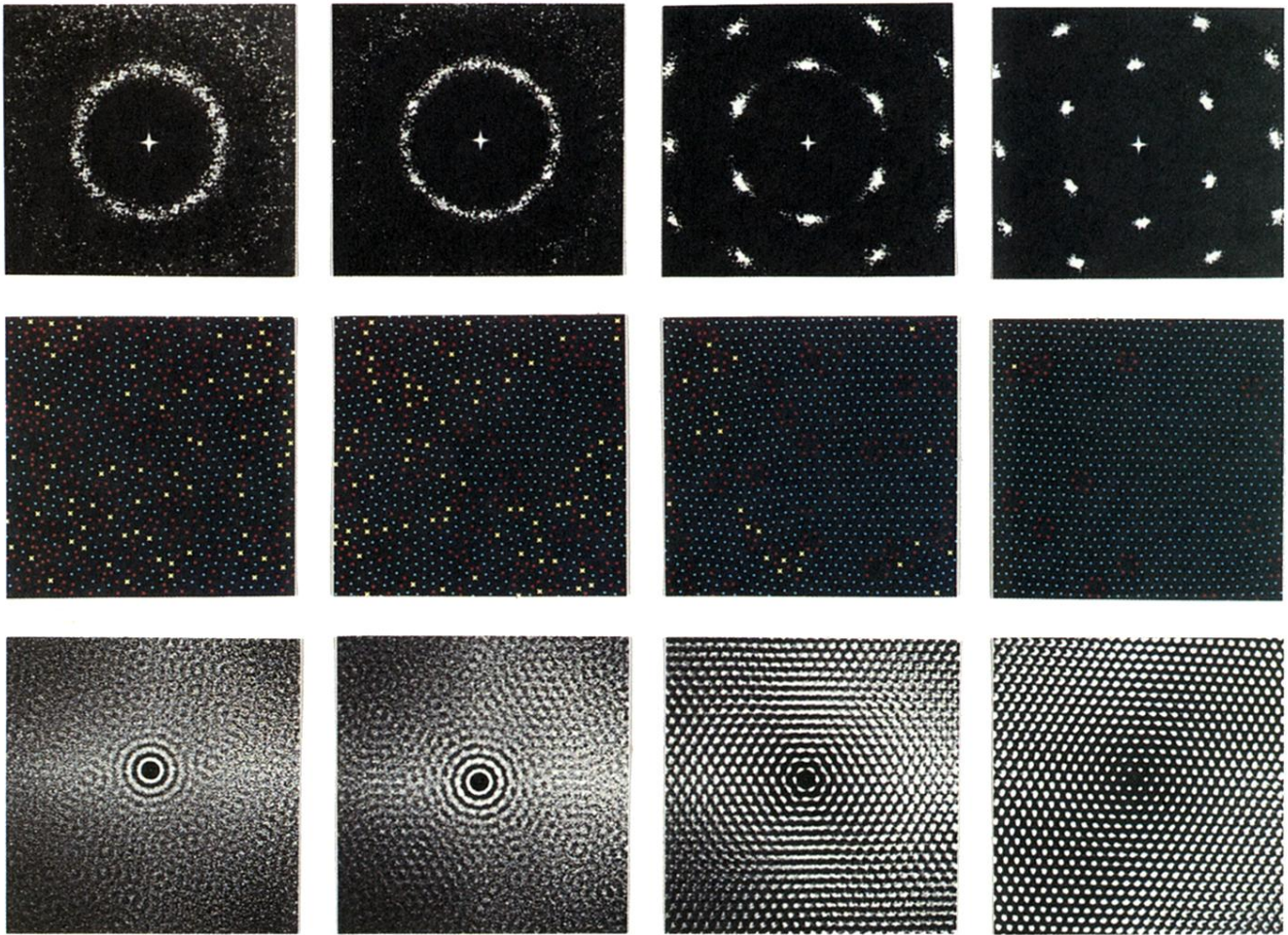
[17]K. J. Strandburg, Phys. Rev. B 34, 3536 (1986).

FIG. 2. Top: $S(K)$; center: locations of sphere centers; bottom: $g(r)$ computed from the series of images corresponding to the labels a, b, d, f in Fig. 1 with the density increasing left to right. For clarity, only about half of the complete image field is shown. Colors and shapes of the symbols used to represent sphere centers indicate their coordination as determined from a Voronoi polyhedron analysis. Blue diamond: 6, small red x: 5, and large yellow x: 7. The distance scales of the center and bottom rows are identical. The nearest-neighbor separations decrease from 0.85 μm to 0.76 μm from left to right.